Model-based deconvolution for dominant, thin-bed seismic reflections

Steve Hearn *
Velseis Pty Ltd and
University of Queensland
steveh@velseis.com.au

Daryn Voss
Velseis Pty Ltd
dvoss@velseis.com.au

SUMMARY

Predictive deconvolution is widely treated as a universally applicable tool for multiple removal and wavelet compression. The fundamental assumption of random reflectivity is seriously compromised in geological situations where the reflection sequence comprises a small number of dominant horizons. This situation is not uncommon in coal environments.

Where the primary seismic objective is high quality imaging of particular target horizons, an improved result can be achieved if the deconvolution is designed according to assumptions more relevant to the geological situation. We outline a simple example of this approach, aimed at imaging a production coal seam, of thickness 5-10 m, at a mine in the Bowen Basin, Australia.

Using horizon time picks from a preliminary volume, the full reflection package associated with the seam is extracted and deterministically filtered to obtain an estimate of the intrinsic wavelet. A Wiener spiking filter, designed on the extracted wavelet, is then used to deconvolve the seam package.

In comparison to the predictive deconvolution approach, this model-based procedure provides improved resolution of the top and base coal interfaces. In addition, derived amplitude and frequency attributes are more robust in terms of known geology. Variants of this simple model-based procedure should have relevance in a range of dominant-horizon situations where predictive deconvolution is invalid.

Key words: model-based deconvolution, thin-bed, coal seismic, resolution.

INTRODUCTION

A fundamental objective of deconvolution is to simplify the reflection package arising at each subsurface interface. Ideally each interface should be represented by a single spike of energy, since this provides optimum resolution of closely spaced horizons.

Short-gap predictive deconvolution is widely treated as a default technique for such wavelet compression. The attractiveness of the method is perhaps due to its ease of use, which relies on a number of inherent assumptions (e.g. Robinson and Treitel, 1980). Firstly, the performance of the deconvolution filter is optimised if the inherent wavelet is minimum delay. Additionally, it is assumed that the overall trace autocorrelation provides an acceptable estimate of the wavelet autocorrelation. This latter requirement is reasonable in geological situations with a significant number of reflecting horizons, of varying contrasts, positioned randomly in depth. A number of well-log analyses have demonstrated that this so called 'random-reflectivity' assumption is violated in many real situations (e.g. Walden and Hosken, 1985; Phythian et al., 1995). In particular, the assumption may be seriously compromised where the geology comprises a small number of dominant reflecting horizons, as is common in coal environments. Under such circumstances, predictive deconvolution may perform poorly as a wavelet compression tool.

MODEL-BASED DECONVOLUTION

We use the term 'model-based deconvolution' generally to describe any deconvolution algorithm which is based on assumptions which are more directly relevant to the specific geology of interest. In this paper we give one simple example of the approach, aimed at imaging a production coal-seam, of thickness 5-10m, at a mine in the Bowen Basin, Australia. Broadly speaking, we exploit *a priori* knowledge of the dominant-seam geology which causes problems with the conventional predictive approach.

Using basic *z*-transform concepts (e.g. Robinson and Treitel, 1980), the impulse response of a single layer can be written as:

$$F(z) = (c_1 + c_2 z^{\delta\tau}) / (1 + c_1 c_2 z^{\delta\tau}) \qquad (1)$$

where c_1 and c_2 are the reflection coefficients at the top and bottom interfaces respectively, and $\delta\tau$ is the two-way time thickness in the layer. This expression incorporates the full filtering effect of the layer, including the primary reflections from the top and base of seam, and all internal multiples. The full seismic reflection package produced by the layer is then given by $P(z) = F(z)W(z)$ where $W(z)$ is the intrinsic seismic wavelet.

In our deconvolution procedure, an estimate of the seismic reflection package, $P(z)$, associated with the target seam is obtained on a shot-by-shot basis. This is done by automatic event alignment and stacking. The intrinsic seismic wavelet can then be recovered as $W(z) = P(z) [F(z)]^{-1}$. In practice, we generally achieve best results using a Wiener estimate of $[F(z)]^{-1}$, rather than using the exact inverse of Equation (1). Physically, this wavelet-estimation stage can be thought of as removal of the base of seam reflector, and all interbed multiples, leaving only the top-of-seam reflection.

Next a Wiener spiking filter is derived for the estimated wavelet, and this filter is applied to all traces in the shot gather. This stage effectively converts the seam reflection package to the spike series defined by $F(z)$. Note that the wavelet spiking operator designed on this target seam can reasonably also be applied throughout the trace

Finally, it seems theoretically desirable to eliminate intrabed multiples, to yield an image comprising only spiked top and base primary reflections. One approach is to design a Wiener filter to convert the layer-response function $F(z)$ to the corresponding multiples-only response. The multiple sequence so derived is then subtracted. Note that this filter is only applicable to the design seam, and not to the whole trace. In practice we have found that this final step provides minimal adjustment, confirming that the interference effects of interbed multiples are of second-order influence, compared to the interaction between the top and base seam events. In the initial real-data trials below we have not included this correction.

Figure 1 confirms the mechanics of the algorithm for a simple synthetic example. Figure 1(a) shows an assumed source wavelet, based on a real shot-record extraction. Figure 1(b) shows the total interference package arising at a seam having two-way time thickness of 6 ms. Figure 1(c) shows the output of the wavelet-estimation stage. This compares well with the starting wavelet of Figure 1(a). A Wiener spiking filter is designed on this wavelet, and applied to the composite of Figure 1(b). As is desirable, the output image (Figure 1(d)) is characterised by a peak corresponding to the top of seam, followed by a trough corresponding to the base of seam. The time positions of the peak and trough correspond well with the input model.

For comparison, Figure 1(e) shows the result of applying a conventional spiking deconvolution to the composite interference package of Figure 1(b). The predictive deconvolution has not provided any simplification of the reflection package. There is some spurious peak splitting due to instability in the derived filter.

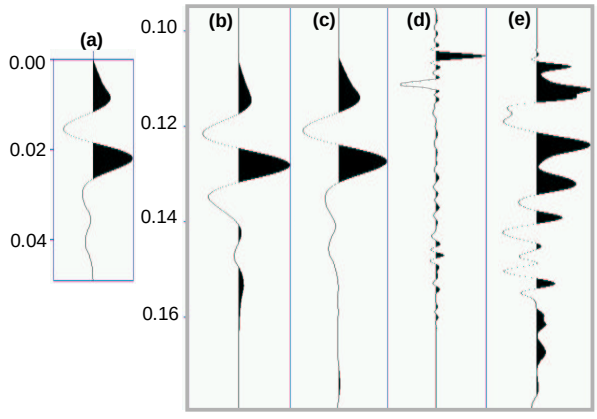

Figure 1. Synthetic illustration of model-based deconvolution: (a) source wavelet based on real data; (b) composite reflection package produced by a seam with a two-way time thickness of 6 ms; (c) wavelet estimate obtained by inverse filtering; (d) output trace obtained by model-based deconvolution of the composite in (b); and (e) output trace obtained by spiking predictive deconvolution of the composite in (b).

ESTIMATION OF MODEL PARAMETERS

As noted above, the model-based approach requires some *a priori* information relating to the target geology. Firstly, Equation (1) indicates that estimates are required of the reflection coefficients at the top and base of the target seam. Consideration of the expansion of $F(z)$ reveals that the ratio c_1 / c_2 is of greater significance than the coefficients themselves. In any event, synthetic analyses suggest that the deconvolution output is relatively insensitive to this ratio. In practice, we have estimated the coefficient ratio from available sonic and density logs. For the real data examples to follow the parameter has been kept constant. There is not a significant change in the output as this ratio is allowed to vary across a reasonable range.

The procedure is much more sensitive to the assumed time-thickness ($\delta\tau$) of the seam, and this parameter must be allowed to vary across the survey area. We have considered a number of approaches to estimating this time-thickness. Figure 2 illustrates an automated procedure referred to here as the relaxation-time approach, which monitors the compression achieved by the deconvolution as the assumed time-thickness is varied. The optimum time-thickness is assumed to yield the most compressed wavelet, as manifested by a minimum in the relaxation time. Figure 2 includes a synthetic example illustrating straightforward estimation of time thickness, and a real-data example where there is some ambiguity associated with multiple minima.

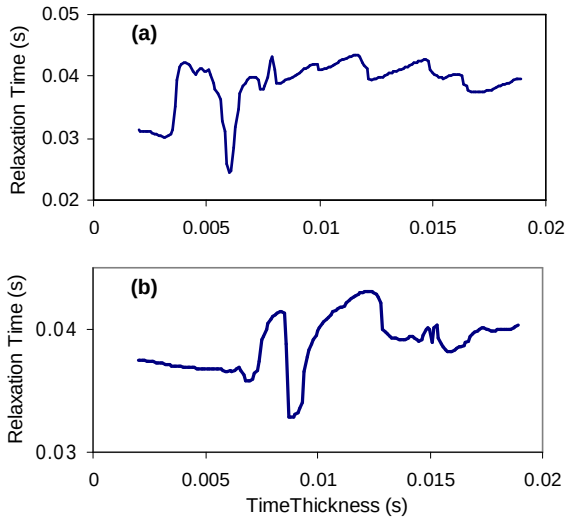

Figure 2. Illustration of relaxation-time analysis for estimation of two-way time thickness of bed. The relaxation time, plotted on the vertical axis, is the time taken for the wavelet partial energy to reach a fixed percentage (typically 90%) of the total energy. For the synthetic example (a), the input model time-thickness was correctly estimated by the clear minimum at 6 ms. For the real data example (b), well logs indicate that the true thickness corresponds to the smaller minimum around 6.5 ms.

The relaxation-time method has potential for fully automated operation on large volume data sets. For the present trial, however, we have restricted ourselves to a more conservative manual approach, whereby we visually examine a panel of deconvolved data, corresponding to a range of assumed time-

thicknesses, at regular locations across the volume. The preferred time-thickness is that which produces best definition on the seam, and least noise generation. This approach is analogous to the panel approach used elsewhere in seismic processing (e.g. filter panels, velocity analysis).

REAL-DATA EXAMPLE

Figure 3(a) shows one receiver-line from a representative 3D shot record, with no deconvolution applied. Polarity considerations imply that the top of seam correlates to the start of the first peak as indicated by the red arrow. This small peak is followed by a stronger trough and peak combination. Figure 3(b) shows the same data following conventional predictive deconvolution. Predictive deconvolution has sharpened each peak or trough, but it has not effectively reduced the overall complexity of the seam reflection package. In this particular case there is some evidence that the initial onset has in fact been made more complex. It is not possible to track the true top-of-seam reflector, although the seam can be structurally mapped by tracking the following trough. Figure 3(c) shows the same data following application of the model-based deconvolution procedure. There is considerable simplification of the reflection package. The dominant peak is now more reliably indicative of the top of seam, while the following trough should more closely relate to base of seam.

The comparative evaluation has been extended to a full 3D test volume. As noted above, in the predictive deconvolution volume the target seam can be effectively tracked on the trough following the true top-of-seam event. Hence, from the point of view of structural mapping, there is no compelling advantage in the new procedure volume. However, for more advanced stratigraphic and quantitative analyses, the model-based volume is considered to provide a more accurate image, since its assumptions are theoretically more defensible. On the target coal seam, definition of the top and base of seam is considerably improved. The improved accuracy of the image is most obvious in various attribute analyses. Figure 4 gives a representative example, where a peak-frequency image of the target seam is displayed for the predictive and model-based deconvolution volumes. On the predictive deconvolution volume (Figure 4(a)) the zones of spuriously high frequency (blue colour) toward the bottom left and right of the figure are difficult to reconcile with known geology. On the other hand, the peak frequencies derived on the model-based volume (Figure 4(b)), are more robust, and can be accurately related to known seam thickness, via tuning arguments (Parker, 2002). Associated attributes (instantaneous frequency, phase) also show greater reliability for the model-based volume.

CONCLUSIONS

Predictive deconvolution is based on certain assumptions which may not be valid in the context of coal seismic reflection. Consequently the conventional technique may not be effective in defining boundaries of relatively thin seams. On the other hand, the model-based algorithm exploits the simplicity of the coal-seam geology, and yields an image with improved definition of the top and base of seam. The model-based procedure requires greater manual intervention than the conventional predictive approach, and requires estimates of seam parameters, most importantly the seam time-thickness. In this trial, thickness was successfully estimated using a simple visual panelling approach.

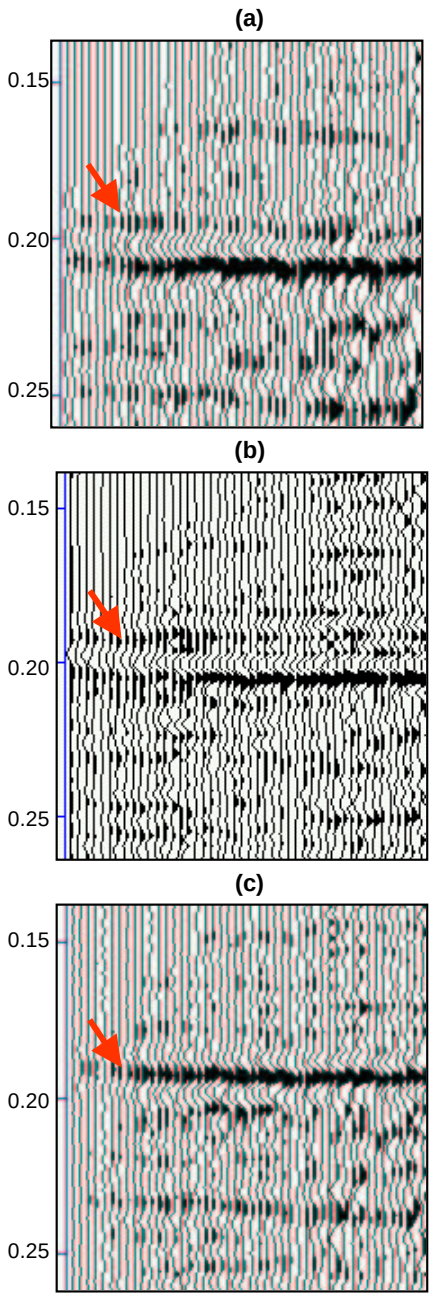

Figure 3. Test data from a single receiver line of a representative 3D shot record. In each image the vertical axis is time in seconds. The approximate top of the production coal seam is indicated by the red arrow. (a) raw data; (b) conventional spiking predictive deconvolution; (c) model-based deconvolution.

In the predictive deconvolution volume, the target seam can be tracked effectively using a trough following the actual top-of-seam peak. Hence, for simple structural mapping there is no compelling argument in favour of the new algorithm. However, for more advanced stratigraphic and quantitative analyses, the model-based volume is considered to provide a more accurate image. Frequency and amplitude attribute images display improved robustness with respect to known geology. In addition, the algorithm should be more amenable to amplitude-sensitive procedures such as impedance inversion. Variants of this simple model-based procedure should have relevance in a range of dominant-horizon situations where predictive deconvolution is invalid.

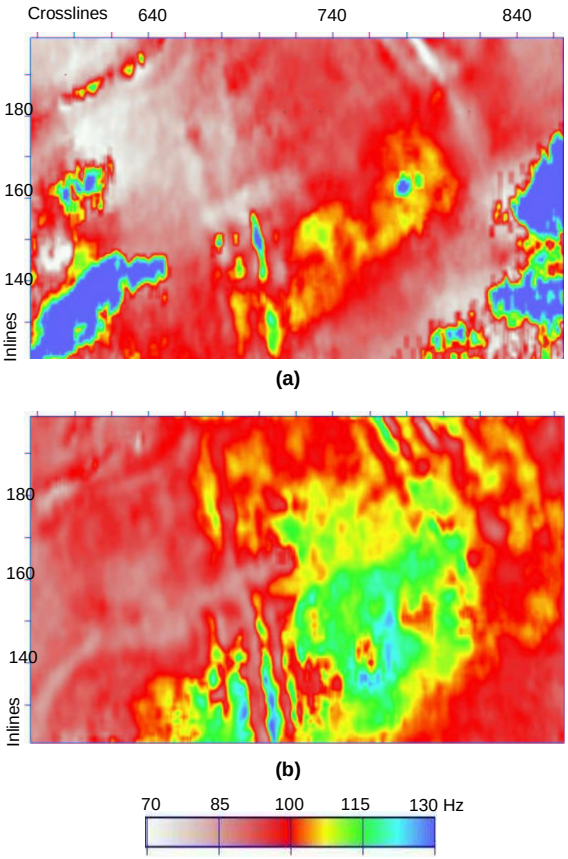

Figure 4. Peak frequency attribute map for (a) predictive deconvolution volume, and (b) model-based deconvolution volume. The analysis was performed using a 30 ms window optimally positioned over the target horizons.

ACKNOWLEDGEMENTS

We acknowledge the support of MIM Exploration and the Newlands Coal Underground Project, and the contributions of Natasha Hendrick (formally MIMEX) and Jason Parker (University of Queensland) for technique evaluation, and 3D attribute analysis, respectively. Seismic Unix, from CWP at Colorado School of Mines, was used for some of the data analysis.

REFERENCES

Parker, J., 2002, Evaluation of frequency attributes for estimation of coal-seam thickness. Honours Thesis, University of Queensland.

Phythian, P., Hearn, S., and Hendrick, N. 1995, Spectral characterisation of reflectivity sequences in the Amadeus, Surat and Bowen Basins, Australia: Exploration Geophysics 26, 497-505.

Robinson E.A. and Treitel S., 1980, Geophysical Signal Analysis: Prentice Hall.

Walden, A.T. and Hosken, J.W.J., 1985, An investigation of the spectral properties of primary reflection coefficients: Geophysical Prospecting 33, 400-435.